FRAMEWORK FOR THE *A POSTERIORI* ERROR ANALYSIS OF NONCONFORMING FINITE ELEMENTS

CARSTEN CARSTENSEN*†, JUN HU‡, AND ANTONIO ORLANDO†

ABSTRACT. This paper establishes a unified framework for the *a posteriori* error analysis of a large class of nonconforming finite element methods. The theory assures reliability and efficiency of explicit residual error estimates up to data oscillations under the conditions **(H1)**-**(H2)** and applies to several nonconforming finite elements: the Crouzeix-Raviart triangle element, the Han parallelogram element, the nonconforming rotated (*NR*) parallelogram element of Rannacher and Turek, the constrained *NR* parallelogram element of Hu and Shi, the P_1 element on parallelograms due to Park and Sheen, and the *DSSY* parallelogram element.

1. INTRODUCTION

Nonconforming finite element methods are very appealing for the numerical approximation of partial differential equations, for they enjoy better stability properties compared to the conforming finite elements. While the study of the approximation properties of nonconforming triangular and quadrilateral elements has reached a certain level of maturity [17, 3, 26], the a posteriori error analysis of nonconforming quadrilateral finite element approximations is still in its infancy.

Following the contribution of [15, 14] the a posteriori error analysis for the L^2 norm of the piecewise gradient of the error, $\|\nabla_h e\|_{L^2(\Omega)}$, has been carried out successfully for triangular elements [9, 1] on the basis of two arguments: (a) the Helmholtz decomposition of $\nabla_h e$ and (b) some orthogonality with respect to some conforming finite element space V_h^c. Condition (b) fails for some quadrilateral nonconforming finite elements, e.g. the nonconforming rotated quadrilateral element of Rannacher and Turek, referred to as *NR* element [24]. As a result, the a posteriori error analysis of $\|\nabla_h e\|_{L^2(\Omega)}$ for nonconforming quadrilateral elements appears as a minefield. For the *NR* element, for instance, the work [22] bypasses condition (b) by some enlargement of V_h^{nc} with local bubble trial functions but their analysis applies only for goal-oriented error control and cannot be extended to the control of $\|\nabla_h e\|_{L^2(\Omega)}$. Another inherent mathematical difficulty for the *NR* element functions results from the non-equivalence of the continuity at midpoints *and* the equality of integral averages along edges. This makes the operator Π in [2] *not* well defined (while correct for all triangular elements of [1]).

This paper aims at some clarification and a unified framework for the *a posteriori* error analysis of nonconforming finite element methods based on properties for parallelogram meshes. The resulting framework is exemplified on the 2D elliptic model

---

problem

(1.1) $\text{div} \nabla u = f$ in Ω, $\quad u = u_D$ on Γ_D, $\quad \nabla u \cdot \nu = g$ on Γ_N,

on some Lipschitz domain $\Omega \subset \mathbb{R}^2$ with the outward unit normal ν along $\partial\Omega :=$ $\Gamma_D \cup \Gamma_N$. Let $V := \{v \in H^1(\Omega) : v = 0 \text{ on } \Gamma_D\}$ denote the space of the test functions approximated by conforming, $V_{h,0}^c$, and nonconforming finite element spaces, $V_{h,0}^{nc}$, associated with a shape regular triangulation $\mathcal{T}$ with $\mathcal{E}$ the set of the edges while $\mathcal{E}(\Omega)$ and $\mathcal{E}(\Gamma_D)$ the interior and boundary edges, respectively. Also, define $[v_h]$ as the jump across $E \in \mathcal{E}(\Omega)$ of the general discontinuous $v_h \in V_h^{nc}$ and $\mathbb{P}_k(\omega)$ the polynomials of total degree k on the domain ω. Throughout the paper, the hypothesis $(\boldsymbol{H1})$-$(\boldsymbol{H2})$ characterize some class of nonconforming finite elements allowing for efficient and reliable error control:

$(\boldsymbol{H1})$ For all $v_h \in V_h^{nc}$ there holds

(1.2) $\displaystyle\int_E [v_h] \, ds = 0$ for $E \in \mathcal{E}(\Omega)$ and $\displaystyle\int_E (v_h - u_D) \, ds = 0$ for $E \in \mathcal{E}(\Gamma_D)$.

$(\boldsymbol{H2})$ There exists some bounded, linear operator $\Pi : V \mapsto V_{h,0}^{nc}$ and some mesh size independent constant C_{stab} with the properties (1.3)-(1.6) for every $v_h \in V_{h,0}^c$, $K \in \mathcal{T}$, and $E \in \mathcal{E}$,

(1.3) $\displaystyle\int_K \nabla w_h \cdot \nabla(v_h - \Pi v_h) \, dx = 0 \quad$ for all $w_h \in V_h^{nc}$;

(1.4) $\displaystyle\int_K q(v_h - \Pi v_h) \, dx = 0 \quad$ for all $q \in \mathbb{P}_1(K)$;

(1.5) $\displaystyle\int_E q(v_h - \Pi v_h) \, ds = 0 \quad$ for all $q \in \mathbb{P}_0(E)$;

(1.6)
$$h_K^{-1}\|v_h - \Pi v_h\|_{L^2(K)} + \|\nabla(v_h - \Pi v_h)\|_{L^2(K)} \leq C_{stab}\|\nabla v_h\|_{L^2(K)}$$
$$h_E^{-1/2}\|v_h - \Pi v_h\|_{L^2(E)} \leq C_{stab}\|\nabla v_h\|_{L^2(\omega_E)}.$$

The main result of the paper (Theorem 3.1 below) establishes the reliability of

(1.7) $\eta^2 \quad := \displaystyle\sum_{K \in \mathcal{T}} \eta_K^2 + \sum_{E \in \mathcal{E}} \eta_E^2, \quad$ with

(1.8) $\eta_K^2 \quad := h_K^2 \|f + \text{div} \nabla u_h\|_{L^2(K)}^2$ for $K \in \mathcal{T}$;

(1.9) $\eta_E^2 \quad := h_E \big(\|J_{E,\nu}\|_{L^2(E)}^2 + \|J_{E,t}\|_{L^2(E)}^2\big)$ for $E \in \mathcal{E}$,

up to the data oscillations $\text{osc}(f)$ and $\text{osc}(g)$ (see Subsection 2.5 below):

(1.10) $\|\nabla_h(u - u_h)\|_{L^2(\Omega)} \leq C_{rel}(\eta + \text{osc}(f) + \text{osc}(g)).$

The weak continuity condition $(\boldsymbol{H1})$ is met by a quite large class of nonconforming finite elements proposed in literature [13, 18, 24, 16, 23, 20]. However, there are also elements that fail the above condition, for instance, the version of the Rannacher-Turek element [24] with local degree of freedom equal to the value of the function

at the midside nodes of each edge, and the nonconforming quadrilateral element of Wilson [28]. Both elements are therefore ruled out by the present analysis.

An outline of the remaining parts of the paper is as follows. Section 2 displays the set-up of the model problem (1.1), introduces the conforming and nonconforming finite element spaces as well as the a posteriori error estimate (1.7) and the data oscillations in (1.10). Theorem 3.1 shows that the abstract conditions **(H1)-(H2)** imply the reliability in the sense of (1.10). This is stated and proved in Section 3 in the abstract frame while the relevant examples follow in Section 4. Namely, applications of the theory are given for the Crouzeix-Raviart element, the Han element [18], the *NR* element [24] with local degrees of freedom equal to the average value over the edges, the constrained nonconforming rotated element of Hu and Shi [20], the P_1 quadrilateral element of Park and Sheen [23], and the *DSSY* element [16]. Finally, some comments on the efficiency, an adaptive finite element method, a numerical example for the *NR* element with hanging nodes, and possible generalizations of (1.1) conclude the paper in Section 5.

2. Notations and Preliminaries

2.1. **Model problem.** Let Ω be a polygonal domain in $\mathbb{R}^2$ with boundary $\Gamma := \partial\Omega$ split into a closed Dirichlet boundary $\Gamma_D \subseteq \Gamma$ with positive surface measure and the remaining Neumann boundary $\Gamma_N := \Gamma \setminus \Gamma_D$. Given $f \in L^2(\Omega)$, $g \in L^2(\Gamma_N)$, $u_D \in H^{1/2}(\Gamma_D)$, and $V := \{v \in H^1(\Omega) : v = 0 \text{ on } \Gamma_D\}$ the solution of (1.1) satisfies

$$(2.1) \qquad \int_\Omega \nabla u \cdot \nabla v \, dx = \int_\Omega f v \, dx + \int_{\Gamma_N} g v \, ds \text{ for every } v \in V \,,$$

where the symbol $\cdot$ is the scalar product in the Euclidean space R^2. Furthermore, we denote by L^2 the Lebesgue space of square integrable functions, and by H^s with $s > 0$ the Sobolev space defined in the usual way [17]. For the corresponding norm we use the symbols $\| \cdot \|_{L^2}$ and $\| \cdot \|_{H^s}$, respectively, with explicit indication of the domain of integration. With Ω an open set of $\mathbb{R}^2$, and $\varphi \in H^1(\Omega)$, the curl- and gradient-operator are given as follows

$$(2.2) \qquad \operatorname{curl}\varphi = (-\partial\varphi/\partial x_2, \, \partial\varphi/\partial x_1), \quad \nabla\varphi = (\partial\varphi/\partial x_1, \, \partial\varphi/\partial x_2) \,,$$

whereas for a $\mathbb{R}^2$-valued function $v = (v_1, v_2)$ the divergence is

$$(2.3) \qquad \operatorname{div} v = \partial v_1/\partial x_1 + \partial v_2/\partial x_2 \,.$$

Throughout the paper, the letter C denotes a generic constant, not neceessarily the same at each occurrence.

2.2. **Conforming finite element spaces.** For approximating (2.1) by the finite element method, we introduce a regular triangulation $\mathcal{T}$ of $\bar{\Omega} \subset \mathbb{R}^2$ in the sense of Ciarlet [11, 6] in closed triangles, or convex quadrilaterals, such that $\bigcup_{K\in\mathcal{T}} K = \bar{\Omega}$, two distinct elements K and K' in $\mathcal{T}$ are either disjoint, or share the common edge E, or a common vertex, that is, hanging nodes are not allowed. Let $\mathcal{E}$ denote the set of all edges in $\mathcal{T}$, and $\mathcal{N}$ the set of the midside nodes m_E of the edges $E \in \mathcal{E}$. The set of interior edges of Ω are denoted by $\mathcal{E}(\Omega)$, the set of edges of the element K by $\mathcal{E}(K)$, whereas those that belong to the Dirichlet and Neumann boundary are

3

denoted by $\mathcal{E}(\Gamma_D)$ and $\mathcal{E}(\Gamma_N)$, respectively. For the set of midpoints of the edges $E \in \mathcal{E}(\Gamma_D)$ we use the notation $\mathcal{N}(\Gamma_D)$. By h_K and h_E we denote the diameter of the element $K \in \mathcal{T}$ and of the edge $E \in \mathcal{E}$, respectively. Also, we denote by ω_K the patch of elements $K' \in \mathcal{T}$ that share an edge with K, and by ω_E the patch of elements having in common the edge E. Given any edge $E \in \mathcal{E}$ we assign one fixed unit normal ν_E; if (n_1, n_2) are its components, t_E denotes the orthogonal vector of components $(-n_2, n_1)$. For $E \in \mathcal{E}(\Gamma_D) \cup \mathcal{E}(\Gamma_N)$ on the boundary we choose $\nu_E = \nu$, the unit outward normal to Ω, and concordingly the tangent versor t. Once ν_E and t_E have been fixed on E, in relation to ν_E one defines the elements $K_{in} \in \mathcal{T}$ and $K_{out} \in \mathcal{T}$, with $E = K_{out} \cap K_{in}$, as depicted in Figure 1.
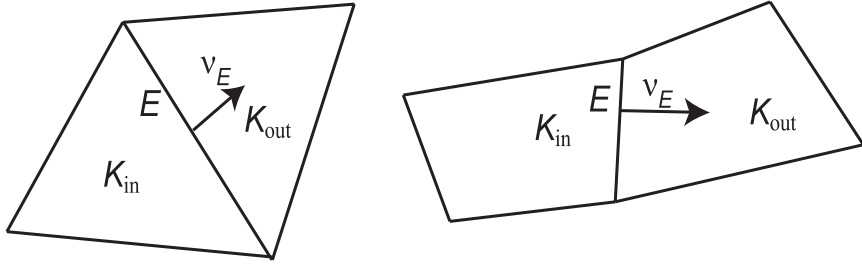

FIGURE 1. Definition of the elements K_{in} and K_{out} in relation to ν_E

Given $E \in \mathcal{E}(\Omega)$ and a $\mathbb{R}^d$-valued function v defined in Ω, with $d = 1, 2$, we denote by $[v]_E$ the jump of v across E, that is,

$$[v]_E(x) = (v|_{K_{out}}(x) - v|_{K_{in}}(x)) \quad \text{for } x \in E = K_{in} \cap K_{out},$$

with the subscript E that will be omitted whenever it is clear from the context. With the triangulation $\mathcal{T}$ we associate, moreover, the space $H^1(\mathcal{T})$ defined as

$$H^1(\mathcal{T}) = \{v \in L^2(\Omega) : \forall K \in \mathcal{T}, v|_K \in H^1(K)\},$$

and for $v \in H^1(\mathcal{T})$, we denote by $\nabla_h v$ the gradient operator defined piecewise with respect to $\mathcal{T}$, i.e.,

$$\nabla_h v|_K := \nabla(v|_K).$$

Whenever from the context it is clear that we are considering the restriction of v to an element $K \in \mathcal{T}$, then we clearly write only ∇v in lieu of $\nabla_h v$.

For a non negative integer k the space $Q_k(\omega)$ consists of polynomials of total degree at most k defined over ω in the case $\omega = K$ is a triangle, whereas it denotes polynomials of degree at most k in each variable in the case K is a quadrilateral. For this presentation it will suffice to assume $k = 1$. The corresponding conforming space will be denoted by

$$V_h^c := \{v \in H^1(\Omega) : v|_K \in Q_1(K)\} \text{ and } V_{h,0}^c := \{v \in V_h^c : v = 0 \text{ on } \Gamma_D\}.$$

Throughout the paper, for triangular elements, $V_{h,0}^c$ stands for the conforming space of P_1 elements, whereas for quadrilateral elements it denotes the conforming space of bilinear elements.

Given the conforming finite element space $V_{h,0}^c$, we consider the Clément interpolation operator or any other regularized conforming finite element approximation

4

operator $\mathcal{J} : H^1(\Omega) \mapsto V_h^c$ with the property

$$(2.4) \qquad \|\nabla \mathcal{J}\varphi\|_{L^2(K)} + \|h_K^{-1}(\varphi - \mathcal{J}\varphi)\|_{L^2(K)} \leq C \|\nabla\varphi\|_{L^2(\omega_K)},$$

$$(2.5) \qquad \|h_E^{-1/2}(\varphi - \mathcal{J}\varphi)\|_{L^2(E)} \leq C \|\nabla\varphi\|_{L^2(\omega_E)},$$

for all $K \in \mathcal{T}$, $E \in \mathcal{E}$, and $\varphi \in H^1(\Omega)$. The existence of such operators is guaranteed, for instance, in [12, 25, 7, 5].

2.3. Nonconforming finite element spaces and a posteriori error estimator.
A nonconforming finite element approximation is defined by a finite dimensional trial space $V_h^{nc} \subset H^1(\mathcal{T})$ along with the test space $V_{h,0}^{nc}$ corresponding to the discrete homogeneous Dirichlet boundary conditions. The nonconforming finite element approximation $u_h \in V_h^{nc}$ of (2.1) then satisfies

$$(2.6) \qquad \int_\Omega \nabla_h u_h \cdot \nabla_h v_h \, dx = \int_\Omega f v_h \, dx + \int_{\Gamma_N} g v_h \, ds \text{ for every } v_h \in V_{h,0}^{nc}.$$

The Helmholtz decomposition is a well-established tool in the a posteriori error analysis of nonconforming finite element methods [15, 9].

Lemma 2.1. *Given any $e \in V + V_h^{nc}$ such that $\nabla_h e \in L^2(\Omega; \mathbb{R}^2)$ there exist w, $\varphi \in H^1(\Omega)$ with $w = 0$ on Γ_D, and $\nabla \varphi \cdot t = \operatorname{curl}\varphi \cdot \nu = 0$ on Γ_N such that*

$$(2.7) \qquad \nabla_h e = \nabla w + \operatorname{curl}\varphi,$$

$$(2.8) \qquad \|\nabla_h e\|_{L^2(\Omega)}^2 = \|\nabla w\|_{L^2(\Omega)}^2 + \|\operatorname{curl}\varphi\|_{L^2(\Omega)}^2. \quad \square$$

2.4. A posteriori error estimator.
For each edge $E \in \mathcal{E}$, define $J_{E,\nu}$ the jump of $\nabla_h u_h$ across E in direction ν_E, i.e.,

$$(2.9) \qquad J_{E,\nu} := \begin{cases} [\nabla_h u_h]_E \cdot \nu_E & \text{if } E \in \mathcal{E}_\Omega, \\ g - \nabla u_h \cdot \nu & \text{if } E \in \mathcal{E}_N, \\ 0 & \text{if } E \in \mathcal{E}_D, \end{cases}$$

and $J_{E,t}$ the jump of $\nabla_h u_h$ across E in direction t_E, i.e.,

$$(2.10) \qquad J_{E,t} := \begin{cases} [\nabla_h u_h]_E \cdot t_E & \text{if } E \in \mathcal{E}_\Omega, \\ 0 & \text{if } E \in \mathcal{E}_N, \\ (\nabla u_D - \nabla u_h) \cdot t & \text{if } E \in \mathcal{E}_D, \end{cases}$$

and recall η from (1.7) with the local contributions η_K (1.8) and η_E (1.9) for each $K \in \mathcal{T}$ and $E \in \mathcal{E}$, respectively.

2.5. Data oscillations.
For $f \in L^2(\Omega)$ and its piecewise affine approximation f_h with respect to $\mathcal{T}$, we refer to $\operatorname{osc}(f)$ as oscillation of f [27],

$$(2.11) \qquad \operatorname{osc}^2(f) := \sum_{K \in \mathcal{T}} h_K^2 \|f - f_h\|_{L^2(K)}^2.$$

with $\operatorname{osc}(f)$ being a higher order term if $f \in H^1(\Omega)$. Similar definitions hold for the oscillations $\operatorname{osc}(u_D)$ and $\operatorname{osc}(g)$ of the Dirichlet and Neumann boundary data, $u_D \in$

$H^{1/2}(\Gamma_D)$ and $g \in L^2(\Gamma_N)$, and their piecewise affine and constant approximations $u_{D,h}$ and g_h, respectively, as [27, 8]

$$\text{osc}^2(u_D) := \sum_{E \in \mathcal{E}(\Gamma_D)} h_E \| \frac{\partial}{\partial s}(u_D - u_{D,h}) \|^2_{L^2(E)},$$

$$\text{osc}^2(g) := \sum_{E \in \mathcal{E}(\Gamma_N)} h_E \| g - g_h \|^2_{L^2(E)}.$$

3. Reliability of η

This section presents the main result of this paper, that is, **(H1)-(H2)** imply reliability of η. Throughout this section, let u solve (2.1), u_h solve (2.6), and set $e := u - u_h$.

Theorem 3.1. *Asssume that the space V_h^{nc} along with the corresponding $V_{h,0}^{nc}$ satisfy **(H1)-(H2)**. Then, there esists a positive constant C depending only on the minimum angle of $\mathcal{T}$ such that η is reliable in the sense that*

$$(3.1) \qquad \|\nabla_h e\|_{L^2(\Omega)} \leq C(\eta + \text{osc}(f) + \text{osc}(g)).$$

The remainder of this section is devoted to the proof of Theorem 3.1. Here and throughout f_h and g_h denote piecewise affine and constant approximations of f and g, respectively. From **(H2)** and for every $v_h \in V_{h,0}^c$, there holds

$$(3.2) \qquad \int_\Omega \nabla_h u_h \cdot \nabla v_h \, dx = \int_\Omega f \Pi v_h \, dx + \int_{\Gamma_N} g \Pi v_h \, ds.$$

Lemma 3.2. *There exists a mesh size independent constant C such that, for every $v_h \in V_{h,0}^c$, there holds*

$$(3.3) \qquad \int_\Omega \nabla_h e \cdot \nabla v_h \, dx \leq C(\text{osc}(f) + \text{osc}(g)) \|\nabla v_h\|_{L^2(\Omega)}.$$

Proof. From (2.1) and (3.2), for every $v_h \in V_{h,0}^c$ it follows

$$\int_\Omega \nabla_h e \cdot \nabla v_h \, dx = \sum_{K \in \mathcal{T}} \left(\int_K (f - f_h)(v_h - \Pi v_h) \, dx + \int_K f_h(v_h - \Pi v_h) \, dx \right)$$

$$+ \sum_{E \in \mathcal{E}(\Gamma_N)} \left(\int_E (g - g_h)(v_h - \Pi v_h) \, ds + \int_E g_h(v_h - \Pi v_h) \, ds \right).$$

Since (1.4)-(1.5), this equals to

$$\int_\Omega (f - f_h)(v_h - \Pi v_h) \, dx + \int_{\Gamma_N} (g - g_h)(v_h - \Pi v_h) \, ds.$$

The combination of Cauchy inequalities with (1.6) yield its upper bound

$$C \left(\left(\sum_{K \in \mathcal{T}} h_K^2 \| f - f_h \|^2_{L^2(K)} \right)^{1/2} + \left(\sum_{E \in \mathcal{E}(\Gamma_n)} h_E \| g - g_h \|^2_{L^2(E)} \right)^{1/2} \right) \|\nabla v_h\|_{L^2(\Omega)}. \qquad \square$$

Remark 3.1. *If $V_{h,0}^c$ is a subspace of $V_{h,0}^{nc}$, then **(H1)**-**(H2)** hold for $\Pi = I$ and (3) recovers the L^2-orthogonality of $\nabla_h e$ and ∇v_h for every $v_h \in V_{h,0}^c$ [because $C = 0$ in (1.6)].*

The following orthogonality condition (3.4) is well established in the literature on a posteriori error estimates for nonconforming finite element schemes.

Lemma 3.3. *For every $v_h \in V_h^c$ such that $\partial v_h / \partial s = 0$ on Γ_N, there holds*

$$(3.4) \qquad \int_\Omega \nabla_h e \cdot \operatorname{curl} v_h \, dx = 0 \,.$$

Proof. The proof is along the lines of [15, eq. (3.4)] for the Crouzeix-Raviart element. An integration by parts over each element gives

$$(3.5) \qquad \int_\Omega \nabla_h e \cdot \operatorname{curl} v_h \, dx = \sum_{E \in \mathcal{E}} \int_E [u - u_h] \frac{\partial v_h}{\partial s} \, ds \,.$$

Since for $v_h \in V_h^c$, $\partial v_h / \partial s$ is constant over each edge $E \in \mathcal{E}(\Omega) \cup \mathcal{E}(\Gamma_D)$, or is zero on $E \in \mathcal{E}(\Gamma_N)$, accounting for **(H1)**, one obtains (3.4). $\qquad\square$

The proof of (3.1) starts with the decomposition (2.7) and the interpolation operator $\mathcal{J}$ of Clément, and Lemma 3.3. Without loss of generality one can choose φ in (2.7) to be equal to a constant on Γ_N, and $\mathcal{J}\varphi|_{\Gamma_N} = \varphi|_{\Gamma_N}$. Then, it follows that

$$\|\nabla_h e\|_{L^2(\Omega)}^2 = \int_\Omega \nabla_h e \cdot (\nabla w + \operatorname{curl} \varphi) \, dx = \int_\Omega \nabla_h e \cdot \nabla(w - \mathcal{J}w) \, dx$$

$$+ \int_\Omega \nabla_h e \cdot \operatorname{curl}(\varphi - \mathcal{J}\varphi) \, dx + \int_\Omega \nabla_h e \cdot \nabla \mathcal{J}w \, dx \,.$$

From Lemma 3.2 and the estimate (2.4), one obtains

$$(3.6) \qquad \begin{aligned} \int_\Omega \nabla_h e \cdot \nabla \mathcal{J}w \, dx &\leq C\big(\operatorname{osc}(f) + \operatorname{osc}(g)\big)\|\nabla \mathcal{J}w\|_{L^2(\Omega)} \\ &\leq C\big(\operatorname{osc}(f) + \operatorname{osc}(g)\big)\|\nabla w\|_{L^2(\Omega)} \,. \end{aligned}$$

Since $(w - \mathcal{J}w)$ and $(\varphi - \mathcal{J}\varphi)$ belong to $H^1(\Omega)$, the use of the Stokes theorem and Green's formula over each element give, after some rearrangements,

$$\int_\Omega \nabla_h e \cdot \nabla(w - \mathcal{J}w) \, dx + \int_\Omega \nabla_h e \cdot \operatorname{curl}(\varphi - \mathcal{J}\varphi) \, dx$$

$$= \sum_{E \in \mathcal{E}} \Big(\int_E J_{E,t}(\varphi - \mathcal{J}\varphi) \, ds + \int_E J_{E,\nu}(w - \mathcal{J}w) \, ds \Big)$$

$$+ \sum_{K \in \mathcal{T}} \int_K (f + \operatorname{div} u_h) \, (w - \mathcal{J}w) \, dx \,.$$

It is a standard argument with Cauchy inequalities and (2.4)-(2.5) to bound this by

$$C\eta\big(\|\nabla w\|_{L^2(\Omega)} + \|\nabla \varphi\|_{L^2(\Omega)}\big),$$

7

with η from (1.7). The combination of the aforementioned estimates with (2.8) concludes the proof of (3.1).

4. EXAMPLES

In this section, we verify **(H1)**-**(H2)** for several nonconforming finite elements proposed in literature. For the following examples, the operator Π that enters **(H2)** is the interpolation operator of V associated with $V_{h,0}^{nc}$.

4.1. The Crouzeix-Raviart element.
The nonconforming finite element space associated with the Crouzeix-Raviart element [13] reads

$$(4.1) \quad V_h^{nc} := \big\{ \ v_h \in H^1(\mathcal{T}) : v_h|_K \in P_1(K) \quad \forall K \in \mathcal{T}, v_h \text{ is continuous at each}$$

$$m_E \in \mathcal{N} \setminus \mathcal{N}(\Gamma_D)\,, \text{ and } v_h(m_E) = u_D(m_E) \text{ for } m_E \in \mathcal{N}(\Gamma_D)\big\}$$

and $V_{h,0}^{nc}$ denotes the space corresponding to the discrete homogeneous Dirichlet boundary conditions. For this element, it is trivial to check that the space V_h^{nc} meets **(H1)**. Furthermore, since $V_{h,0}^c \subset V_{h,0}^{nc}$, **(H2)** follows immediately and Theorem 3.1 recovers the results of [15, 9].

4.2. The Han element.
With respect to the global coordinate system (x_1, x_2), the nonparametric formulation of rectangular and parallelogram elements proposed by Han in [18] is obtained by introducing the following local space

$$(4.2) \qquad \mathcal{Q}_{\mathcal{H}}^{nc} = \text{span}\{ 1, x_1, x_2, x_1^2 - \frac{5}{3}x_2^4, x_2^2 - \frac{5}{3}x_1^4 \}\,,$$

and the $\mathcal{Q}_{\mathcal{H}}^{nc}$-unisolvent set of linearly independent linear forms [11, 18] read

$$(4.3) \quad \mathcal{F}_E(v) = \frac{1}{h_E} \int_E v \, ds\,, \quad \mathcal{F}_K(v) = \frac{1}{|K|} \int_K v \, dx \text{ with } E \in \mathcal{E}(K)\,, \quad K \in \mathcal{T}.$$

This defines the five degrees of freedom for the Han element. In (4.3), $|K|$ denotes the area of the element. Recall from [11] that given $E = K \cap K'$ for $K, K' \in \mathcal{T}$, and $v \in H^1(\mathcal{T})$ such that $v|_K \in \mathcal{Q}_{\mathcal{H}}^{nc}(K)$, and $v|_{K'} \in \mathcal{Q}_{\mathcal{H}}^{nc}(K')$, we say that v is continuous with respect to $\mathcal{F}_E$ if $\mathcal{F}_E(v|_K) = \mathcal{F}_E(v|_{K'})$. The nonconforming finite element space V_h^{nc} is then defined as

$$(4.4)$$
$$V_h^{nc} := \big\{ v \in H^1(\mathcal{T}) : v|_K \in \mathcal{Q}_{\mathcal{H}}^{nc}(K) \text{ for each } K \in \mathcal{T}, v \text{ continuous with respect}$$

$$\text{to } \mathcal{F}_E \text{ for all } E \in \mathcal{E}(\Omega)\,, \text{ and } \mathcal{F}_E(v) = \mathcal{F}_E(u_D) \text{ for all } E \in \mathcal{E}(\Gamma_D)\big\}\,,$$

whereas $V_{h,0}^{nc}$ denotes the space corresponding to the discrete homogeneous Dirichlet boundary conditions in (4.4). For $v_h \in V_h^{nc}$, the definition (4.4) of V_h^{nc} and (4.3) yield

$$(4.5) \quad \int_E [v_h] \, ds = 0 \text{ for all } E \in \mathcal{E}(\Omega) \text{ and } \int_E (v_h - u_D) \, ds = 0 \text{ for all } E \in \mathcal{E}(\Gamma_D)\,,$$

and so V_h^{nc} verifies **(H1)**. Let V_h^c be the conforming space of the bilinear elements constructed from the local spaces $\mathcal{Q}^c(K) = \text{span}\{1, x_1, x_2, x_1 x_2\}$. Consider then the interpolation operator $\Pi : V \mapsto V_{h,0}^{nc}$ defined by the conditions: For all $E \in \mathcal{E}(K)$

8

and $K \in \mathcal{T}$,

$$(4.6) \qquad \Pi v \in V_{h,0}^{nc}, \quad \mathcal{F}_E(\Pi v|_K) = \mathcal{F}_E(v|_K), \quad \mathcal{F}_K(\Pi v|_K) = \mathcal{F}_K(v|_K).$$

Given $v \in V_{h,0}^c$, the restriction of v to $K \in \mathcal{T}$ has the following representation

$$(4.7) \qquad v = a_0 + a_1 x_1 + a_2 x_2 + a_3 x_1 x_2,$$

for some interpolation constants a_i, $i = 0, \ldots, 3$. Since the degrees of freedom (4.3) vanish over the bubble function $x_1 x_2 \in \mathcal{Q}^c(K)$, it follows that the restriction of Π to $V_{h,0}^c$ yields

$$(4.8) \qquad \Pi v|_K = a_0 + a_1 x_1 + a_2 x_2.$$

Using standard estimates for polynomial approximations, one can easily verify that Π meets the estimates (1.6). Furthemore, for every $v_h \in V_{h,0}^c$ a direct evaluation of the integrals shows (1.3)-(1.5) over rectangular and parallelogram element domains, i.e., the space V_h^{nc} meets $(\boldsymbol{H2})$.

4.3. **The quadrilateral rotated nonconforming element.** In [24] Rannacher and Turek introduce two types of quadrilateral nonconforming elements referred to as *NR* element. The corresponding local finite element spaces are obtained by rotating the mixed term of the bilinear element, and assuming as local degree of freedom either the average of the function over the edge or its value at the midside node. In this section we consider the non parametric formulation for rectangular and parallelogram elements with the first choice of degree of freedom. More precisely, for each element $K \in \mathcal{T}$ and with respect to the global coordinate system (x_1, x_2), we set [24]

$$(4.9) \qquad \mathcal{Q}_{\mathcal{R}}^{nc} = \mathrm{span}\{\, 1,\, x_1,\, x_2,\, x_1^2 - x_2^2 \,\},$$

and introduce the four degree of freedom as [11, 24]

$$(4.10) \qquad \mathcal{F}_E(v) = \frac{1}{h_E} \int_E v \, ds \text{ with } E \in \mathcal{E}(K).$$

With the corresponding nonconforming finite element space defined as in (4.4) and concordingly $V_{h,0}^{nc}$, it follows that V_h^{nc} meets $(\boldsymbol{H1})$.

For any $v \in V$, the interpolation operator $\Pi v \in V_{h,0}^{nc}$ is defined as [24, 20]: For all $E \in \mathcal{E}(K)$, and $K \in \mathcal{T}$

$$(4.11) \qquad \Pi v \in V_{h,0}^{nc} \text{ and } \mathcal{F}_E(\Pi v|_K) = \mathcal{F}_E(v|_K)$$

hence, likewise the Han element, since $\mathcal{F}_E$ vanishes over the bubble function $x_1 x_2 \in \mathcal{Q}^c(K)$, the restriction of Π to $V_{h,0}^c \subset V$ is represented locally by (4.8). Therefore, the above arguments verify $(\boldsymbol{H2})$.

Remark 4.1. *For the version of the NR element with function evaluation at the midpoints as degree of freedom, $(\boldsymbol{H1})$ is not satisfied and we refer to Section 4.5 for a modification of the NR element.*

Remark 4.2. *The proof of Lemma 3.3 for the NR element can be found in [19, 21].*

Remark 4.3. *The interpolation operator $\Pi_{\mathcal{P}}$ defined in [2, eq. (6)] does, in general, not map into the space $X_{\mathcal{P},E}$ of the NR element functions continuous at the midside*

nodes [2, page 4]. *This results in a gap in the analysis of* [2] *for this finite element; the remaining assertions in* [2] *seem to be correct.*

Remark 4.4. *The present analysis shows that the augmentation of V_h^{nc} with local bubble trial functions proposed in* [22] *is not necessary for the error control of $\|\nabla_h e\|$; this proves a conjecture in* [22].

4.4. **The constrained NR element and the P_1-quadrilateral element.** The constrained rotated nonconforming finite element (referred to as CNR element) introduced in [19, 20] is obtained by enforcing a constraint on the degree of freedom of the NR element described in Section 4.3. With $\mathcal{Q}_{\mathcal{R}}^{nc}$ denoting here the space of the global trial functions defined over Ω and corresponding to the NR element, the space of the CNR element is then defined as follows

(4.12)
$$\mathcal{Q}_{\mathcal{J}}^{nc} := \left\{ v \in \mathcal{Q}_{\mathcal{R}}^{nc} : \forall K \in \mathcal{T} \int_{E_1} v \, ds + \int_{E_3} v \, ds = \int_{E_2} v \, ds + \int_{E_4} v \, ds \right.$$

$$\left. \text{with } E_i \quad 1 \leq i \leq 4 \text{ edges of } K \in \mathcal{T} \text{ numbered in counterclockwise order} \right\}.$$

For rectangular and parallelogram element domains, here considered, the element is equivalent to the P_1-quadrilateral element of [23]. For homogeneous Dirichlet boundary conditions, it is trivial to check that the space V_h^{nc} meets $(\boldsymbol{H1})$, for being the CNR space a subspace of NR. Furthermore, in [19, 20] it is also proved that on the generic element $K \in \mathcal{T}$ with vertices 1, 2, 3, 4 labelled in counterclockwise, the interpolation $\Pi v \in V_{h,0}^{nc}$ defined as in (4.11) and for $v \in V_{h,0}^c$ has the following representation

(4.13)
$$\Pi v|_K = v_1 \phi_1 + v_2 \phi_2 + v_3 \phi_3 + v_4 \phi_4$$

with v_i nodal value of $v \in V_{h,0}^c$ and

$$\phi_1(x_1, x_2) = \frac{1}{4}(1 - x_1 - x_2), \quad \phi_2(x_1, x_2) = \frac{1}{4}(1 - x_1 + x_2),$$

(4.14)

$$\phi_3(x_1, x_2) = \frac{1}{4}(1 + x_1 + x_2), \quad \phi_4(x_1, x_2) = \frac{1}{4}(1 - x_1 + x_2),$$

associated with each of such vertices. The arguments of Section 4.3 show $(\boldsymbol{H2})$.

4.5. **The $DSSY$ element.** The main motivation for the definition of this element is to obtain a quadrilateral element with approximation properties similar to that of the Crouzeix-Raviart element. For parallelogram elements these properties were identified in [16] by (i) continuity at the midpoints of each edge, (ii) value of the function at these points as degrees of freedom, and (iii) validity of the orthogonality condition [16, eq. (6.1)]: For all $v_h \in V_{h,0}^{nc}$ there holds

(4.15)
$$\int_E [v_h] \, ds = 0 \text{ for } E \in \mathcal{E}(\Omega).$$

The latter condition plays a crucial role in the proof of optimal error estimates as realized in [16], for instance, by two spaces of local basis obtained by an *ad hoc*

modification of the local basis of the Rannacher-Turek element. Set

$$(4.16) \qquad \theta_\ell(t) = \begin{cases} t^2 - \frac{5}{3}t^4 & \text{for } \ell = 1, \\ t^2 - \frac{25}{6}t^4 + \frac{7}{2}t^6 & \text{for } \ell = 2. \end{cases}$$

Then the local space reads

$$(4.17) \qquad \mathcal{Q}_\mathcal{D}^{nc} = \mathrm{span}\{1, x_1, x_2, \theta_\ell(x_1) - \theta_\ell(x_2)\} \quad \text{for } \ell = 1, 2,$$

and the $\mathcal{Q}_\mathcal{D}^{nc}$-unisolvent linear forms read

$$(4.18) \qquad \mathcal{F}_{E_i}(v_h|_K) = v_h|_K(m_{E_i}) \text{ for } E_i \in \mathcal{E}(K), \, 1 \le i \le 4, \, v_h \in \mathcal{Q}_\mathcal{D}^{nc},$$

with m_{E_i} midside nodes of the edge E_i. The nonconforming finite element spaces V_h^{nc} and $V_{h,0}^{nc}$ are then defined as in (4.4) with $\mathcal{Q}_\mathcal{H}^{nc}$ replaced by $\mathcal{Q}_\mathcal{D}^{nc}$. Following [16], one can show that $(\boldsymbol{H1})$ holds. Furthermore, with the interpolation operator $\Pi : V \mapsto V_{h,0}^{nc}$ defined as in (4.11), one obtains

$$(4.19) \quad \Pi v \in V_{h,0}^{nc}, \quad \Pi v|_K(m_E) = \frac{1}{h_E} \int_E v \, ds \text{ for each edge } E \in \mathcal{E}(K), \quad K \in \mathcal{T},$$

with the restriction of Π to the space $V_{h,0}^c$ having the local representation (4.8) that implies $(\boldsymbol{H2})$.

5. COMMENTS

This section concludes the paper with remarks on extensions and generalizations.

5.1. Efficiency.
The efficiency of η in the sense that there exists a mesh size independent constant C such that

$$(5.1) \qquad \eta \le C(\|\nabla_h e\|_{L^2(\Omega)} + \mathrm{osc}(f) + \mathrm{osc}(u_D) + \mathrm{osc}(g)).$$

follows from the local bounds

$$\eta_K^2 \le C\left(\|\nabla_h e\|_{L^2(\omega_K)}^2 + h_K^2 \|f - f_h\|_{L^2(\omega_K)}^2 \right) \text{ for each } K \in \mathcal{T};$$

$$(5.2) \qquad \eta_E^2 \le C\left(\|\nabla_h e\|_{L^2(\omega_E)}^2 + h_E^2 \|f - f_h\|_{L^2(\omega_E)}^2 + h_E \|g - g_h\|_{L^2(E \cap \Gamma_N)}^2 \right.$$

$$\left. + h_E \|\frac{\partial}{\partial s}(u_D - u_{D,h})\|_{L^2(E \cap \Gamma_D)}^2 \right) \text{ for each } E \in \mathcal{E}.$$

For the proofs, one can adapt the arguments from [27, page 15-18] and [15, 9, 8].

5.2. Adaptive finite element method.
By rewriting η from (1.7) as $\eta^2 = \sum_{K \in \mathcal{T}} \eta_K^2$ with

$$\eta_K^2 := h_K^2 \|f + \mathrm{div}\, u_h\|_{L^2(K)}^2 + \frac{1}{2} \sum_{E \in \mathcal{E}(K)} h_E \left(\|J_{E,\nu}\|_{L^2(E)}^2 + \|J_{E,t}\|_{L^2(E)}^2 \right),$$

the estimate η and the elemental contributions η_K can be used to generate the triangulations $\{\mathcal{T}_\ell\}_{\ell \in \mathbb{N}}$ in an adaptive way using the following Algorithm 1

Algorithm 1. *Input a coarse mesh $\mathcal{T}_0$ with rectangular elements, and set $\ell = 0$.*
(a) Solve the discrete problem on $\mathcal{T}_\ell$ with N degrees of freedom.

11

(b) Compute η_K for all $K \in \mathcal{T}_\ell$ and $\eta_N := (\sum_{K \in \mathcal{T}} \eta_K^2)^{1/2}$.
(c) Mark $K \in \mathcal{M} \subset \mathcal{T}_\ell$ for refinement into four congruents rectangles if $\theta \max_{T \in \mathcal{T}_\ell} \eta_T \leq \eta_K$.
(d) Mark further elements to ensure at most one hanging node per edge. Define the resulting mesh as the actual mesh $\mathcal{T}_{\ell+1}$, update ℓ and go to (a).

The triangulations $\mathcal{T}$ generated by the Algorithm 1 are $1-$irregular meshes [4], i.e. at most one hanging node per edge; it remains open whether the analysis can be extended to hanging nodes. Error reduction and convergence of the adaptive finite element method based on the bulk criterion has very recently been established in [10] for the Crouzeix-Raviart element.

5.3. **Numerical example.** On the $L-$shaped domain $\Omega = [0, 1]^2 \setminus [0.5, 1.0]^2$, we use the $N\!R$ element defined in Section 4.3 to approximate the Poisson's problem (1.1) with $f \equiv 0$, $\Gamma_D = \partial\Omega$, $\Gamma_N = \emptyset$, and u_D a smooth function such that in polar coordinates

$$u(r, \theta) = r^{2/3}\sin(\frac{2}{3}\theta)$$

is the exact solution of (1.1). Figure 2 displays experimental convergence rates for the exact error and the estimate η_N, for uniform and adaptive refinement with the corresponding triangulations depicted in Figure 3. The adaptive refinement improves the convergence rate of uniform refinement to the optimal one $O(N^{-1/2})$ with respect to the number of degrees of freedom, and the convergence rate of the estimate mirrors the one of the exact error both for uniform and adaptive refinement. The boundeness of $\eta_N/\|\nabla_h e_N\|$ observed in Figure 2 conjectures the reliability of η_N also for hanging nodes.

5.4. **Generalizations.** If $A \in L^\infty(\Omega; \mathbb{R}^{2\times2})$ denotes a symmetric positive definite matrix piecewise constant with respect to $\mathcal{T}$, then Theorem 3.1 with corresponding modifications for the definition of η applies also to the elliptic PDE div $A\nabla u = f$ with boundary conditions $u = u_D$ on Γ_D and $(A\nabla u) \cdot \nu = g$ on Γ_N.

References

[1] M. Ainsworth, Robust a posteriori error estimation for nonconforming finite element approximation, *Preprint*, University of Strathclyde (2003)

[2] M. Ainsworth, A posteriori error estimation for non-conforming quadrilateral finite elements, Int. J. of Numerical Analysis and Modeling, 2 (2005) 1–18

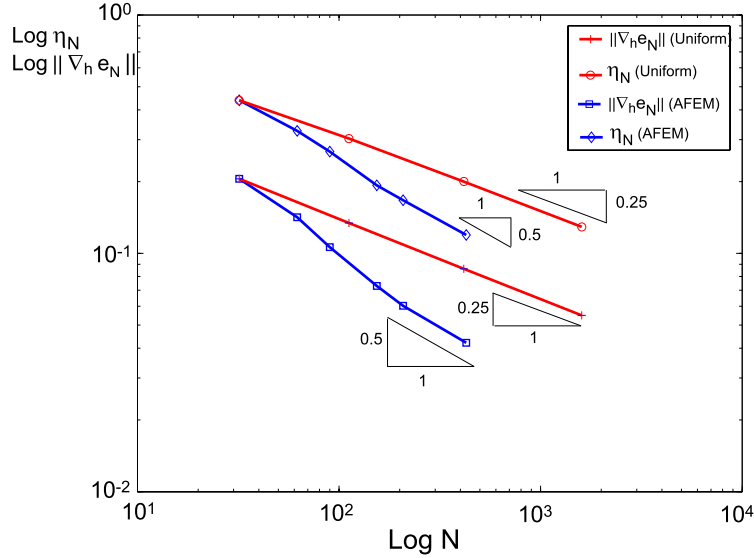[3] D.N. Arnold, D. Boffi, R.S. Falk, Approximation by quadrilateral finite elements, Math. Comp. 71 (2002) 909–922

FIGURE 2. Experimental convergence rate of η_N and the exact error $\|\nabla_h e_N\|$ with respect to the number N of degrees of freedom for the adaptive and uniform refinement based on η_N and with the *NR* finite element. The displayed results show $2.13 \leq \eta_N/\|\nabla_h e_N\| \leq 2.83$ for adaptive and $2.13 \leq \eta_N/\|\nabla_h e_N\| \leq 2.35$ for uniform mesh refinement.

[4] I. Babuska, A. Miller, A feedback finite element method with a posteriori error estimation: Part I. The finite element method and some basic properties of the a posteriori error estimator, Comp. Meth. Appl. Mech. Engrg. 61 (1987) 1–40

[5] C. Bernardi, V. Girault, A local regularisation operator for triangular and quadrilateral finite elements, SIAM J. Numer. Anal. 35 (1998) 1893–1916

[6] S.C. Brenner, L.R. Scott, *The Mathematical Theory of Finite Element Methods.* Springer Verlag, 2*nd* Edition, 2002

[7] C. Carstensen, Quasi-interpolation and a posteriori error analysis in finite element methods, M2AN Math. Model. Numer. Anal. 33 (1999) 1187–1202

[8] C. Carstensen, S. Bartels, Each averaging technique yields reliable a posteriori error control in FEM on unstructured grids. Part I: Low order conforming, nonconforming, and mixed FEM, Math. Comp. 71 (2002) 945-969

[9] C. Carstensen, S. Bartels, S. Jansche, A posteriori error estimates for nonconforming finite element methods, Numer. Math. 92 (2002) 233–256

[10] C. Carstensen, R.H.W. Hoppe, Convergence analysis of an adaptive nonconforming finite element method, *Preprint* (2005)

[11] P.G. Ciarlet, *The Finite Element Method for Elliptic Problems.* North–Holland, 1978; reprinted as SIAM Classics in Applied Mathematics, 2002

[12] P. Clément, Approximation by finite element functions using local regularization, RAIRO Anal. Numér. 9 (1975) 77–84

[13] M. Crouzeix, P.-A. Raviart, Conforming and nonconforming finite element methods for solving the stationary Stokes equations, RAIRO Anal. Numér. 7 (1973) 33–76

[14] E. Dari, R. Duran, C. Padra, Error estimators for nonconforming finite element approximations of the Stokes problem, Math. Comp. 64 (1995) 1017–1033

[15] E. Dari, R. Duran, C. Padra, V. Vampa, A posteriori error estimators for nonconforming finite element methods, M^{2}AN 30 (1996) 385–400

[16] J. Douglas Jr, J.E. Santos, D. Sheen, X. Ye, Nonconforming Galerkin methods based on quadrilateral elements for second order elliptic problems, M2AN Math. Model. Numer. Anal. 33 (1999) 747–770

[17] V. Girault, P.-A. Raviart, *Finite Element Methods for Navier–Stokes Equations*, Springer Verlag, 1986

[18] Hou-De Han, Nonconforming elements in the mixed finite element method, J. Comp. Math., 2 (1984) 223–233

[19] Jun Hu, Quadrilateral locking free elements in elasticity, *Doctorate Dissertation (in Chinese)*, Institute of Computational Mathematics, Chinese Academy of Science (2004)

[20] Jun Hu, Zhong-Ci Shi, Constrained nonconforming rotated Q_1-element, *to appear in J. Comp. Math.*

[21] Jun Hu, Zhong-Ci Shi, Analysis of nonconforming-nonconforming quadrilateral rotated Q_1 element for Reissner-Mindlin plate, *Preprint* $2003-10$, Institute of Computational Mathematics, Chinese Academy of Science (2003)

[22] G. Kanschat, F.-T. Suttmeier, A posteriori error estimates for nonconforming finite element schemes, Calcolo 36 (1999) 129–141

[23] C. Park, D. Sheen, $P1$-nonconforming quadrilateral finite element methods for second-order elliptic problems, SIAM J. Numer. Anal. 41 (2003) 624-640

[24] R. Rannacher, S. Turek, Simple nonconforming quadrilateral Stokes element, Num. Meth. PDE 8 (1992) 97–111

[25] L. R. Scott, S. Shang, Finite element interpolation of nonsmooth functions satisfying boundary conditions, Math. Comp. 54 (1990) 483–493

[26] Zhong-Ci Shi, The F-E-M test for convergence of nonconforming finite elements, Math. Comp. 49 (1987) 391–405

[27] R. Verfürth, *A Review of A Posteriori Error Estimation and Adaptive Mesh-Refinement Techniques*, Wiley–Teubner, 1996

[28] E.L. Wilson, R.L. Taylor, W. Doherty, J. Ghaboussi, Incompatible displacement models. In S.J. Fenves, N. Perrone, A.R. Robinson, W.C. Schnobrich, editors, *Numerical and Computer Methods in Structural Mechanics* 43-57. Academic Press, 1973.

† INSTITUT FÜR MATHEMATIK, HUMBOLDT UNIVERSITÄT ZU BERLIN, RUDOWER CHAUSSEE 25, D–12489 BERLIN, GERMANY

‡ INSTITUTE OF COMPUTATIONAL MATHEMATICS, CHINESE ACADEMY OF SCIENCES, NO. 55, ZHONG-GUAN-CUN DONG LU, BEIJING 100080, CHINA.
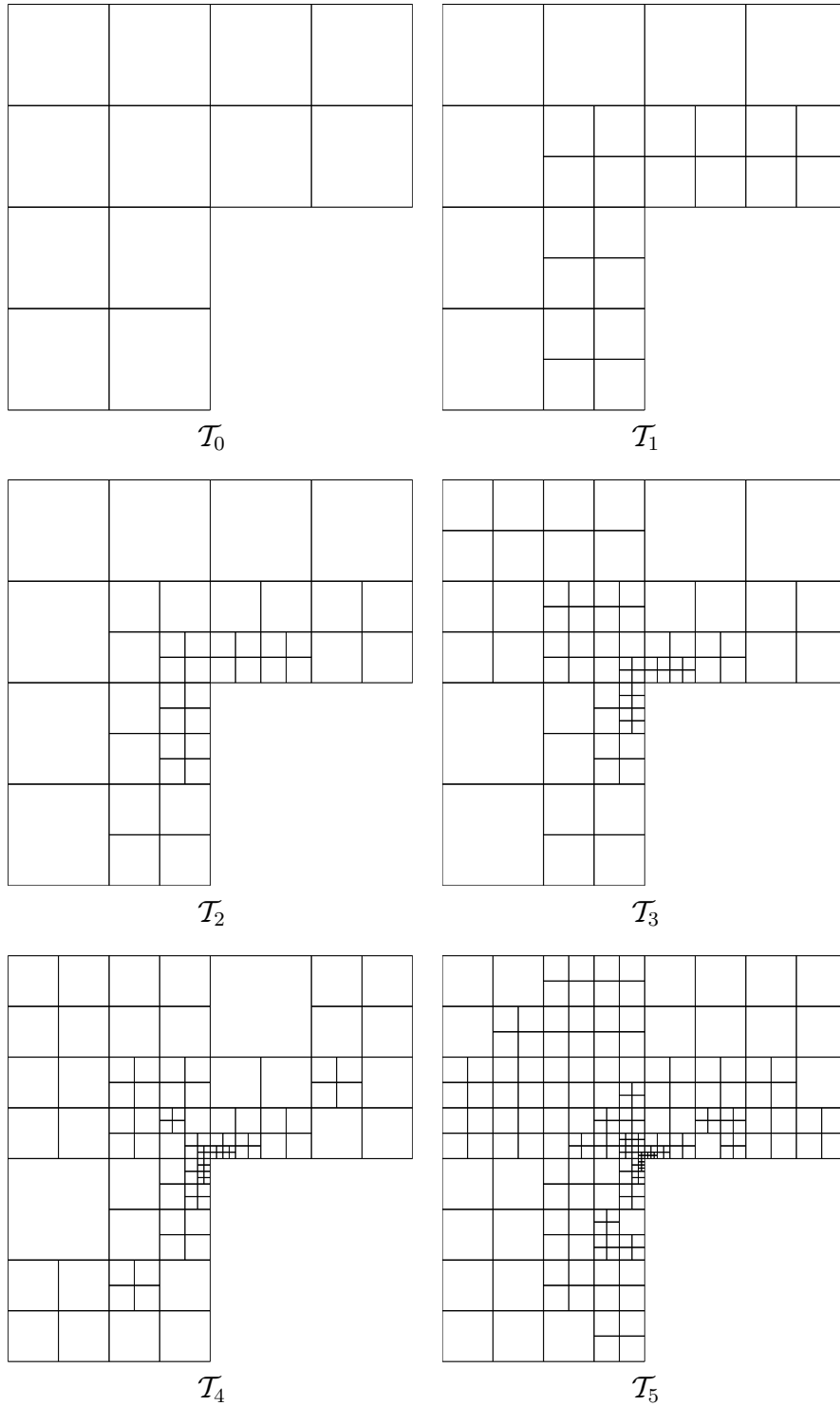
$\mathcal{T}_0$

$\mathcal{T}_1$

$\mathcal{T}_2$

$\mathcal{T}_3$

$\mathcal{T}_4$

$\mathcal{T}_5$

FIGURE 3. Adapted triangulations $\mathcal{T}_0, \ldots, \mathcal{T}_5$ generated with the Algorithm 1 with $\theta = 1/2$. Notice a local higher refinement towards the reentrant corner.

15